Traveling Wave-Based Fault Locators: Performance Analysis in Series-Compensated Transmission Lines

R. L. A. Reis, F. V. Lopes, E. P. Ribeiro, C. M. Moraes, K. M. Silva, A. M. Britto,
R. L. Agostinho, M. A. M. Rodrigues

***Abstract*—In this paper, the performances of one-ended and two-ended traveling wave (TW)-based fault location techniques in series compensated transmission lines (SCTLs) are thoroughly investigated, highlighting the impact of the series capacitors (SCs) and their associated overvoltage protection on such routines. To do so, a diversity of fault simulations were carried out on a realistic Alternative Transients Program (ATP) power system model of a 500 kV/60 Hz double-circuit SCTL located in the north region of Brazil. From the carried out studies, it is demonstrated that the two-ended algorithm is not impacted when the SCs are installed at the line ends, but the single-ended routines based on correlation functions are more affected by the SCs banks, even though some promising results may be obtained depending on their adjustments.**

***Keywords*—Correlation-based functions, fault location, series capacitors, transmission lines, traveling waves, two-ended methods.**

I. Introduction

With the continuous technological advances and the increasing use of electronic-based loads, the customers have become more sensitive to outages. In this context, reliable fault location functions are typically required to speed up the supply restoration process and guarantee a high-quality customer service [1], in which the class of traveling wave (TW)-based fault locators currently appears as one of most robust ways to pinpoint the short-circuit distance [2].

Despite it is well-known the robustness of two-ended TW-based fault location methods due to the need of detecting only the first fault-induced incident waves [3], studies and solutions on one-terminal TW-based techniques have been intensified in the last years. Such alternatives are developed to provide economic and accurate fault location estimations without requiring communication means nor time-stamping synchronization devices [4].

Most of the TW-based fault location algorithms are designed to properly work in non-compensated transmission lines (TLs) [2], [5]–[7]. On the other hand, to improve the power transfer capability in order to meet the energy demand growth, utilities have increasingly installed series capacitors (SCs) on longer lines, in such a way that fault location solutions for series-compensated transmission lines (SCTLs) have been a target of interest of companies and researches worldwide [8], [9]. Theoretically, the presence of capacitive elements should not be a cause for concern since TW-based applications require higher frequency components as input data, in which the capacitive elements typically behave as short-circuits for such frequency spectrum, providing a low impedance path to the surges move along. However, in SCTLs, the performance of the SC overvoltage protection may introduce some challenges in the fault location process, specially due to the non-linear characteristics of the metal oxide varistors (MOVs) and/or air gaps [1], [10].

Some double-ended TW-based fault location techniques for SCTLs are reported in the literature [9], [11]–[13]. In such situations, different equations are derived according to the SCs locations, which are chosen depending on a previous faulty section identification routine. On the other hand, to allow applications in cases in which failures on the time-stamping synchronization process may take place, a single-terminal TW-based fault location method for SCTLs is proposed in [14], but the fault locator needs to be placed at the SC point, which may limit its deployment in real-world applications due to economic reasons. Besides, its applicability is restricted considering the SC installed only at the middle of the line.

Other one-terminal TW-based routines have been reported over the years. For example, single-ended correlation-based TW fault location (SEC-TWFL) methods were one of the first solutions to distinguish fault-induced reflected from refracted surges [15], [16], but the impact of low frequencies and difficulties to properly set their parameters have limited their application in the past. In this scenario, hybrid methods have gained space [17], [18], but the limiting factors of impedance-based fault locators may impact on the proper identification of reflected waves [19]. As a result, studies on SEC-TWFL techniques have reappeared due to signal processing advances, and some solutions were recently proposed [5], [7]. However, such methods were applied only in non-compensated lines, in such a way that their performances on SCTLs are still unknown.

From the literature review, although few TW-based fault location methods for SCTLs are reported in the literature, most of them are concerned to two-terminal applications. For one-ended techniques, a scarcity of solutions is evident, even such subject being of prime importance for SCTLs operation and maintenance. Besides, the techniques are usually

This work was developed in partnership with IATI and CEPEL within the scope of the R&D project PD-06908-0003/2021, sponsored by ANEEL and EVOLTZ.

R. L. A. Reis and F. V. Lopes are with Federal University of Paraíba (UFPB), Brazil (email: raphael.leite, felipelopes@cear.ufpb.br). E. P. Ribeiro, C. M. Moraes, K. M. Silva and A. M. Britto are with University of Brasília (UnB), Brazil (email: eduardopassos, caiomoraes, klebermelo, amaurigm@lapse.unb.br). R. L. Agostinho is with Evoltz, Brazil (email: rodrigo.lehnemann@evoltz.com.br). M. A. M. Rodrigues is with CEPEL, Brazil (email: mamr@cepel.br).

Paper submitted to the International Conference on Power Systems Transients (IPST2023) in Thessaloniki, Greece, June 12-15, 2023.

validated considering simple power system topologies that may not hold true in real-world applications, and they may not take into account detail modeling of the SC associated protection as well. As a consequence, questions about the real performances and challenges of single-ended TW-based fault location functions in SCTLs are still not completely answered, especially because there is a scarcity of works that investigate in detail such subjects.

Therefore, thorough analysis regarding the performance and viability on the use of three different SEC-TWFL methods in SCTLs are addressed in this paper, pointing out the impact of the SC and its associated protection on the correlation functions. To do so, fault simulations are carried out on an Alternative Transients Program (ATP) power system model of a 500 kV/60 Hz double-circuit SCTL located in the north region of Brazil, and then investigated in detail to address the challenges and some potential ways to apply them in SCTL fault location applications. To allow comparative analysis, a classical two-ended TW-based fault location technique is also taken into account.

II. Theory Background

A. Series Compensation

Capacitors installed in series with the TLs are commonly used to reduce the line equivalent reactance, which brings out some benefits to the grid, such as increasing the power transfer capability and improving the system stability. However, in short-circuit situations, the SCs are subject to fault-induced transients, in such a way that their associated protections need to limit possible overvoltages in the SCs terminals [8], [10].

The SC protection is usually performed by the MOV (connected in parallel with the capacitor bank), which is a nonlinear resistance that behaves as an open-circuit for normal operation, and as a low resistance path for fault conditions that result in voltage values above a predefined threshold. As a consequence, the loading current flows through the SCs in steady-state operation (i_{SC}), whereas a part of it is deviated through the MOV (i_{MOV}) in case of disturbances in the TL to limit the SC voltage. Protection schemes monitor the MOV accumulated energy level to bypass the capacitor bank if it exceeds a given value. On the other hand, air gaps may be also included to protect the MOV. In such cases, if the MOV energy level is exceeded, the gap flashover, deviating i_{MOV} and bypassing the SCs [10]. A schematic representation of a SC associated protection including MOV and gap is presented in Fig. 1.

To illustrate the performance of the SC associated protection, an AG fault located at 5 km away from the monitored bus (Lechuga substation) of the power system described in section III is carried out, whose i_{SC}, i_{MOV} and the instant of gap flashover are shown in Fig. 2.

As presented in Fig. 2, i_{SC} is deviated through the MOV as long as its predefined voltage threshold is exceeded. As a consequence, the MOV accumulated energy starts to increase up to its limit, which triggers the air gap and causes the SC to be bypassed.

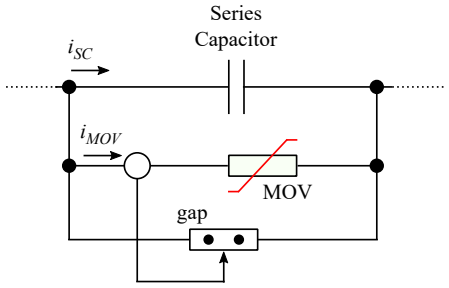

Fig. 1. Schematic representation of a fixed SC bank and its associated protection.

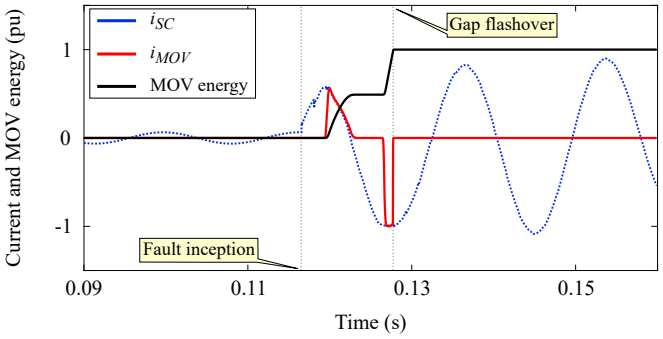

Fig. 2. MOV accumulated energy, i_{mov} and gap flashover due to an AG fault at 5 km away from the monitored bus.

B. TW-Based Fault Location Techniques

To better understand the TW-based fault location principles, consider the simplified network depicted in Fig. 3, in which a fault occurs at a distance d (point F) from the monitored terminal of a ℓ km long TL. In such context, fault-induced TWs go forth and back along the line until they are completely damped.

One-ended TW-based fault location techniques depend on the time delay (τ) between the fault-induced incident wave (at time t_1) and its correspondent reflected surge (at time t_3). To estimate such delay, SEC-TWFL methods take advantage of the fault-generated wave shape patterns, in which a correlation process of the forward (S_f) and backward (S_b) signals provides the τ value when the best match between these S_f and S_b waveforms takes place, since it is expected that incident and reflect surges present similar wave shapes [15].

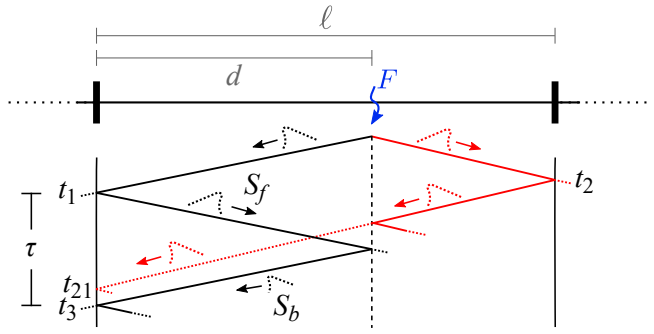

Fig. 3. Simplified power network.

The relaying signals S_f and S_b are derived from the solutions of a lossless TL differential equations, which are [1]:

$$V(x,t) = f_f\left(t - \frac{x}{\upsilon}\right) + f_b\left(t + \frac{x}{\upsilon}\right), \quad (1)$$

$$I(x,t) = \frac{1}{Z_s}\left[f_f\left(t - \frac{x}{\upsilon}\right) - f_b\left(t + \frac{x}{\upsilon}\right)\right], \quad (2)$$

being V and I the aerial mode voltage and current signals at a distance x of the TL, respectively, f_f and f_b the forward and backward TW relaying waveforms, respectively, t is the time, υ is the TW speed, and Z_s is the line surge impedance. As a result, S_f and S_b can be computed from (1) and (2) as:

$$S_f = V(x,t) + Z_s I(x,t) = 2 \cdot f_f\left(t - \frac{x}{\upsilon}\right), \quad (3)$$

$$S_b = V(x,t) - Z_s I(x,t) = 2 \cdot f_b\left(t + \frac{x}{\upsilon}\right). \quad (4)$$

The correlation function (φ) is computed considering sampled windows of S_f and S_b signals, in which a section of length Δk of S_f is stored as a template, which is designed to contain the complete TW information about the first wavefronts. This template signal is correlated with delayed sampled windows of S_b as a function of τ, according to [5]:

$$\varphi(\tau) = \frac{1}{\Delta k}\sum_{k=1}^{\Delta k} S_b(k\Delta t + \tau) \cdot S_f(k\Delta t), \quad (5)$$

being Δt the sampling period and k the k-th sample.

When the best match between S_f and S_b waveforms occurs, a maximum positive peak is obtained in $\varphi(\tau)$ output, and this τ value can be used to estimate the fault location (d), as [1]:

$$d = \frac{\upsilon \cdot \tau \cdot \Delta t}{2}. \quad (6)$$

Basically, a correlation process is performed in most of the TW-based fault location applications. In fact, it is usual to correlate electrical signals with other types of filtering strategies, assuming as a template some filter coefficients taken from wavelet transform [7] or differentiator-smoother strategy [4], for example. In such cases, the best match between the filter coefficients and the evaluated electrical waveform indicates a TW occurrence. Different from the mentioned solutions, the template signal (filter coefficients) in SEC-TWFL routines are directly taken from the electrical waveforms.

To illustrate the impact of SCs on S_f signals, the same AG fault carried out in section II-A is considered. However, to allow comparative analysis, cases with and without series compensation were taken into account. To do such study, Thévenin equivalents were adjusted at both local (Lechuga) and remote (Silves) substations of the network described in section III in order to maintain the same loading current at steady-state operation in both situations (with and without SCs). The corresponding S_f waveforms are shown in Fig. 4, being S_{fSC} the S_f wave shape for the case with SC and S_f for the case without SC.

As presented in Fig. 4, for cases with installed SCs, the first fault-induced transients are more evident in the S_f signal than in situations without SCs (see zoom area 1 in Fig. 4). In fact, right after a disturbance, the energy stored in the capacitances and the TL inductors may be exchanged to each other, resulting in more apparent TWs. Such information are included in the template signal and correlated with successive delayed S_b waveforms to estimate τ, by using (5). On the other hand, although it is expected that more damped fault-generated transients will be identified as they travel along the TL (which is the case without SCs), other high-frequency components appear as soon as the gap flashover (see zoom area 2 in Fig. 4).

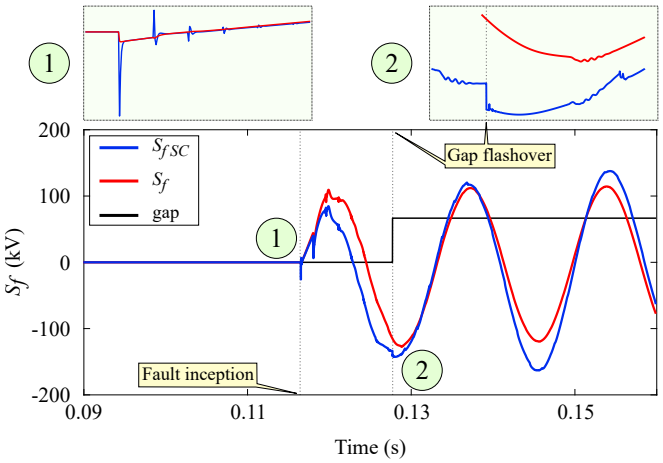

Fig. 4. S_f waveforms for an AG fault considering cases with and without SCs.

In Fig. 5, the S_f signal for the case with SCs as a function of the parameter Δk is presented, in order to demonstrate the template signal according to different Δk values typically used in classical SEC-TWFL techniques, being N the number of samples per cycle [5], [15], [16].

Thus, as shown in Fig. 5, the template signal may not include the transients generated by the performance of the SC associated protection. In this way, the high-frequencies generated when the SCs are bypassed may affect the correlation process, since such components may not be presented in the template S_f signal and they do not bring any information about the fault-induced TWs propagation characteristics.

In this paper, the methods reported in [5], [15] and [16] are considered in the evaluations, which are named as M_1, M_2 and M_3, respectively. Besides, comparative analysis are also carried out with a classical two-ended TW-based algorithm

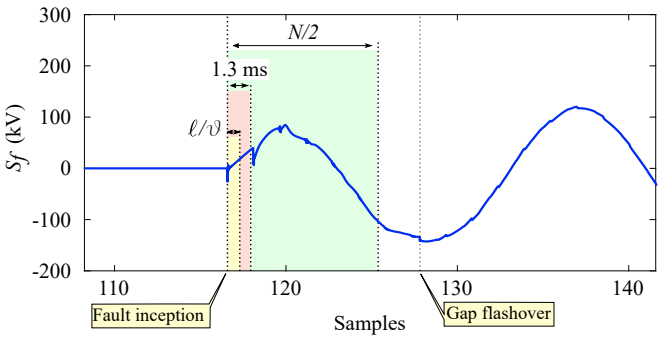

Fig. 5. S_f waveforms as a function of typical Δk values.

(TE-TWFL), whose fault point d is computed as [1]:

$$d = \frac{\ell + (t_1 - t_2) \cdot v}{2} \ . \tag{7}$$

III. Analysis and Results

The performance of SEC-TWFL techniques in SCTLs regarding the impact of SCs and their associated protection is investigated in this section. The TE-TWFL routine is also taken into account to allow comparative analysis. In such cases, it is considered synchronized measurements at both local and remote buses.

A. Test System and Analysis Methodology

Fault simulations were carried out on a power system model of a 500 kV/60 Hz double-circuit SCTL located in the north region of Brazil, whose single-line diagram is presented in Fig. 6. The grid is modeled in ATP/ATPDraw and it consists in the interconnected network upstream 500 kV Lechuga (LEC) substation, the 500 kV double-circuit TLs from LEC through Silves (SIL) up to Tucuruí, the Belo Monte power plant and the DC $\pm$ 800 kV lines connecting Xingu to Estreito and to Terminal Rio. In such power grid, realistic models of SC banks and their associated protection are considered, whose adjustments are set as they are implemented in the field. Static var compensator models are also taken into account.

The circuit 2 of the double-circuit line interconnecting the 500 kV LEC and SIL substations were considered in the short-circuit simulations, which is 223.76 km long with series and shunt compensation at both terminals. The TLs are modeled assuming the JMarti frequency-dependent model and v was determined by a line energization maneuver, resulting in approximately 298,744 km/s. It is worth mentioning that the adjacent lines connecting such substations also consist in double-circuit SCTLs, which brings more complexity to the analysis of the fault-induced transients.

Basically, 72 short-circuit simulations are performed for each considered TW-based fault location technique, but varying their parameters, such as fault location, resistance, inception angle, and type, resulting in an amount of 288 evaluated cases. The faults were applied next to the LEC substation, in the middle of the line and near the SIL substation. The fault simulation variables are shown in Table I.

Since the main goal here is investigating the performance of the TW-based routines and their viability in SCTLs, each setting of the evaluated methods is adjusted from a range of different values reported in the literature, particularly regarding to Δk and to the considered frequency spectrum of S_f and S_b [20]. In this way, in each short-circuit test, Δk and the filtering strategy may be modified to check the methods performances.

In each simulation, voltage and current measurements are recorded and used as input data to the SEC-TWFL techniques, considering a sampling frequency of 1 MHz. For the TE-TWFL routine, voltage samples are also used, following practical applications [21], being the voltage signals measured at the TL side. Although it is well-known the poor frequency

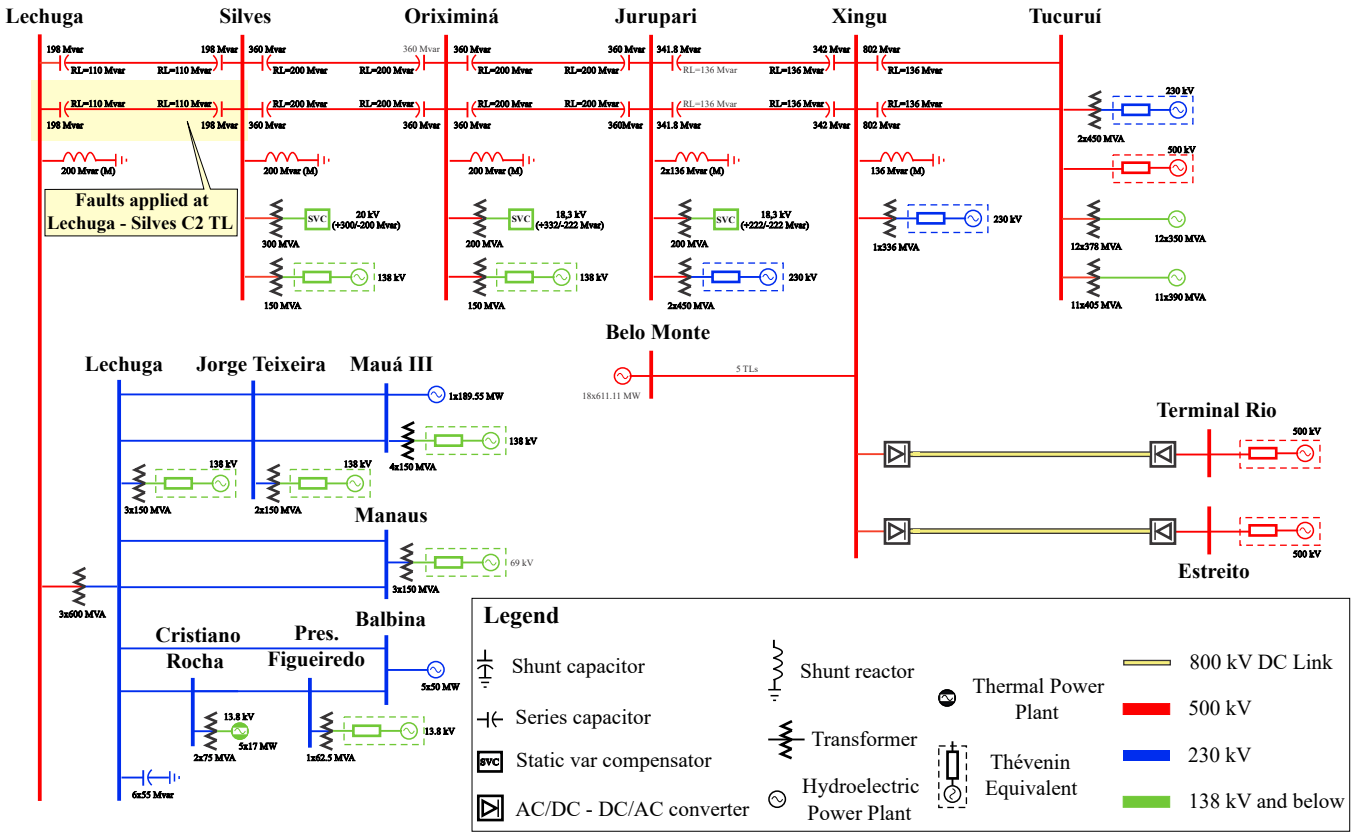

Fig. 6. Single-line diagram of the evaluated 500 kV/60 Hz Brazilian power grid.

TABLE I
FAULT SIMULATION VARIABLES USED IN THE CARRIED OUT ANALYSIS

Simulation variables	Values
Fault location (km)	10, 111.36, 208.34
Fault type	AG, BC, BCG, ABC
Inception angle (°)	30, 60, 90
Fault resistance (Ω)	1, 50

response of conventional coupling capacitor voltage transformers, the researches and practical procedures are going toward the development of solutions to provide high-fidelity voltage measurements for higher frequencies, such as using optical voltage transformers, or by measuring the capacitive stack currents to reconstruct the voltage signal [22]. Thus, it is considered here that voltage measurements with acceptable accuracy are available at the LEC and SIL terminals. The obtained results are computed in terms of the absolute errors, which are estimated according to:

$$\varepsilon = |d - \tilde{d}| \ , \tag{8}$$

being d the actual fault location and $\tilde{d}$ the estimated disturbance point. The obtained errors for the TE-TWFL, M_1, M_2 and M_3 routines are named as ε_{TE}, ε_{M_1}, ε_{M_2} and ε_{M_3}, respectively.

B. Obtained Results and Discussions

Comparing the performance of the TE-TWFL method with the SEC-TWFL techniques, the obtained errors for each evaluated algorithm are presented in Fig. 7, in which ε_{TE} are shown at the y-axis and ε_M at the x-axis. In this context, estimated errors presented in the upper half of the graph (yellow part) indicate higher values of ε_{TE} in relation to ε_M. The opposite holds true for the lower half of the graph (green part). It is worth mentioning that in the following analysis, only errors smaller than approximately three tower spans ($\approx$ 1 km) were considered as convergent results, which is within a typical range of accuracy for TW-based applications. The number of cases in which the estimated errors were above than this threshold (non-convergent cases) for each evaluated method is shown in Table II.

Regarding specifically to the obtained results for the TE-TWFL algorithm, the presence of the SCs at the TL sides and their associated protection did not affect its performance for the evaluated cases. In fact, since the SC typically behaves as a short-circuit for the fault-generated transients that appear right after the disturbance inception, the TWs were properly detected at the LEC and SIL substations, and the estimated errors were within the expected range for such type of technique. Also, no values of non-convergent cases were obtained, as presented in Table II.

TABLE II
NUMBER OF NON-CONVERGENT CASES FOR EACH EVALUATED METHOD

Method	Number of non-convergent cases
TE-TWFL	0
M_1	4
M_2	6
M_3	10

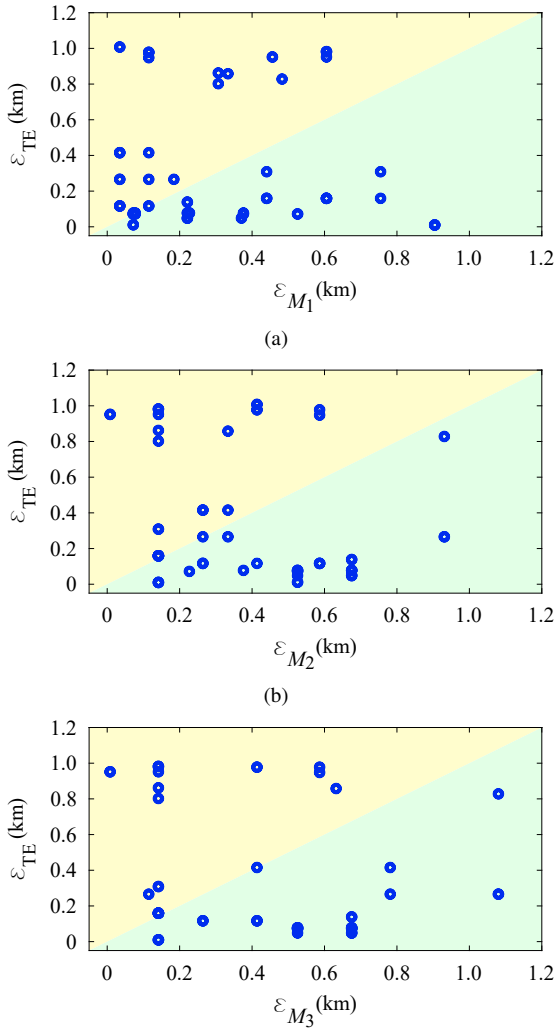

Fig. 7. Comparison between the performances of TE-TWFL and SEC-TWFL techniques: (a) ε_{TE} and ε_{M_1}; (b) ε_{TE} and ε_{M_2}; (c) ε_{TE} and ε_{M_3}.

It is worth mentioning that evaluations carried out here consider the detailed modeling of the real-world power grid shown in Fig. 6, in which the SCs are installed at the line sides, being the obtained results valid for such network configuration. In this way, no tests were carried out considering the SCs located in the middle of the TL.

Considering the results presented in Table II, convergent cases were only estimated by the TE-TWFL techniques, whereas M_1, M_2 and M_3 algorithms presented 4, 6 and 10 non-convergent situations, respectively. Such estimations were obtained considering different adjustments for the M_2 and M_3 techniques, specifically regarding to the length of Δk and the frequency spectrum of S_f and S_b signals. The M_1 algorithm did not need any change in its predefined settings to achieve the estimated results shown here.

The non-convergent fault cases for the SEC-TWFL methods were obtained for short-circuits located far away from the monitored bus, with smaller values of fault inception angles

and higher values of fault resistances. In these cases, since the reflected surges become more damped as they travel along the line, the correlation process may not properly work because the template waveform contains only the highest frequencies in the data window (typically in lengths of ℓ/v or 1.3 ms). Besides, in cases in which the SC associated protection triggers, some transients are also inserted into the measured waveforms, which may affect the correct identification of τ, since such information is not included in the template waveform.

Comparing the performances of the SEC-TWFL techniques with the TE-TWFL routine, as shown in Fig. 7, the M_1 method presented closer results compared to the TE-TWFL algorithm for the evaluated fault scenarios. In this context, the use of a data window length with more samples allows the template signal to have more information about the power grid during the disturbance occurrence, which improves the correlation procedure even if the SC associated protection operates.

To particularly compare the performance of the evaluated SEC-TWFL methods, the obtained errors were plotted as stacked bars in Fig. 8 as a function of the fault type and distances, being figures a, b and c related to the fault inception angles of 30°, 60° and 90°, respectively.

From the obtained results shown in Fig. 8, the smallest errors were estimated by M_1. In fact, such algorithm takes into account higher frequency components of the forward and backward relaying signals, i.e., S_f and S_b waveforms, respectively, and a data window length of $N/2$, which contains more information about the fault-generated transients, which consequently improves the correlation process. On the other hand, M_2 and M_3 may be affected by possible low frequencies that may appear in the forward and backward waveforms, which affect the correlation function in estimating the time delay between the first fault-induced incident and the corresponding reflected surge.

However, M_2 and M_3 routines presented better performance for faults near the monitored terminal, irrespective to the fault type. In these cases, as the highest frequencies are induced by the disturbance and a train of surges are quickly identified at the local bus, the use of smaller data window lengths for the template signal may improve the method performance as well as speed up the correlation process. Even so, the use of a longer data window in such cases guaranteed a reliable and better performance along the line, as demonstrated by the M_1 solution.

Therefore, from the carried out analysis presented in this paper, the use of TW-based fault location solutions typically developed for non-compensated TLs may appear as potential alternatives to be applied in SCTLs, whose results are demonstrated by considering a detailed power system and SCs modeling. As a consequence, the obtained results address the impacts of SCs and their associated protection on TW-based fault location algorithms, especially for single-ended applications, contributing to a subject which is rarely reported in the literature. In this context, promising results may be obtained by single-ended methods in SCTLs as long as studies are carried out to better determine the adjustments of each evaluated algorithm.

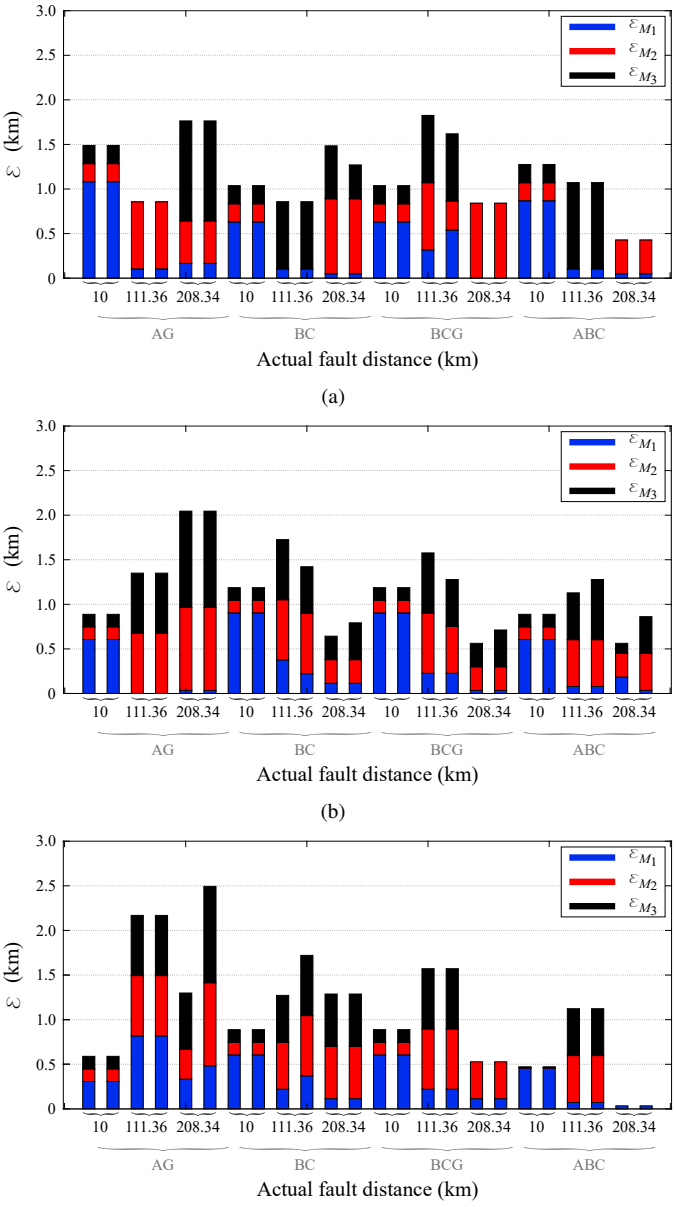

Fig. 8. Stack bars of the obtained errors for the M_1, M_2 and M_3 techniques with a fault inception angle of: (a) 30°; (b) 60°; (c) 90°.

IV. Conclusions

In this paper, the performances of a TE-TWFL and three different SEC-TWFL methods in SCTLs are thoroughly investigated, pointing out the impact of the SCs and their associated protection on TW-based fault location estimations. To do so, short-circuit simulations were carried out on a realistic power system model of a 500 kV/60 Hz double-circuit SCTL located in the north region of Brazil. By considering such a power network, more realistic and complex fault-induced transients are noticed, as the ones generated by the SCs associated overvoltage protection, imposing more challenges to the short-circuit distance estimation procedure.

From the obtained results, the presence of SCs at the line ends do not affect the TE-TWFL routine, as expected since they depend only on the identification of the first incident surges, and typically the capacitors behave as short-circuits for

such high frequency components, providing low-impedance paths to the surges move along.

On the other hand, for some SEC-TWFL fault location functions, the SC associated overvoltage protection may insert some transients into the measured waveforms when it operates, whose frequency components combined with the use of template signals may affect the correlation process in identifying the corresponding fault-induced reflected surge. In fact, the TW patterns induced by the short-circuit chosen as template and the air gap-generated transients superimposed on S_f and S_b signals may have led to unexpected performance on computing the correlation function. However, the use of a longer data window length for the template signal and a higher frequency spectrum of the input data have guaranteed more reliable results for the SEC-TWFL routine, as obtained by the M_1 technique.

Thus, even being originally developed to work in non-compensated TLs, the evaluated TW-based fault location techniques may appear as promising alternative solutions to be applied in SCTLs, whose studies carried out address the challenges faced by such routines in SCTLs, pointing out possible ways to help in the development of more robust functionalities.

V. Acknowledgment

The authors thank the cooperation of Ms. Larissa Silva (EVOLTZ).

References

[1] M. M. Saha, J. Izykowski, and E. Rosolowski, *Fault Location on Power Networks*, ser. Power Systems. London: Ed. Springer, 2010.

[2] F. V. Lopes, R. L. A. Reis, K. M. Silva, A. Martins-Britto, E. P. A. Ribeiro, C. M. Moraes, and M. A. M. Rodrigues, "Past, present, and future trends of traveling wave-based fault location solutions," in *2021 Workshop on Communication Networks and Power Systems (WCNPS)*, 2021, pp. 1–6.

[3] E. O. Schweitzer, A. Guzmán, M. V. Mynam, V. Skendzic, B. Kasztenny, and S. Marx, "Locating faults by the traveling waves they launch," in *2014 67th Annual Conference for Protective Relay Engineers*, March 2014, pp. 95–110.

[4] A. Guzmán, B. Kasztenny, Y. Tong, and M. V. Mynam, "Accurate and economical traveling-wave fault locating without communications," in *2018 71st Annual Conference for Protective Relay Engineers (CPRE)*, March 2018, pp. 1–18.

[5] R. Reis, F. Lopes, W. Neves, D. Fernandes Jr., C. Ribeiro, and G. Cunha, "An improved single-ended correlation-based fault location technique using traveling waves," *International Journal of Electrical Power and Energy Systems*, vol. 132, p. 107167, 2021.

[6] O. D. Naidu and A. K. Pradhan, "Precise traveling wave-based transmission line fault location method using single-ended data," *IEEE Transactions on Industrial Informatics*, vol. 17, no. 8, pp. 5197–5207, 2021.

[7] V. Gonzalez-Sanchez, V. Torres-García, and D. Guillen, "Fault location on transmission lines based on travelling waves using correlation and modwt," *Electric Power Systems Research*, vol. 197, p. 107308, 2021.

[8] H. J. Altuve, J. B. Mooney, and G. E. Alexander, "Advances in series-compensated line protection," in *63rd Annual Georgia Tech Protective Relaying Conference*, March 2009.

[9] O. D. Naidu and A. K. Pradhan, "Model free traveling wave based fault location method for series compensated transmission line," *IEEE Access*, vol. 8, pp. 193 128–193 137, 2020.

[10] P. M. Anderson and R. G. Farmer, *Series Compensation of Power Systems*. USA: PBLSH! Inc., 1996.

[11] Y. Liu, S. Meliopoulos, N. Tai, L. Sun, and B. Xie, "Protection and fault locating method of series compensated lines by wavelet based energy traveling wave," in *2017 IEEE Power and Energy Society General Meeting*, 2017, pp. 1–5.

[12] B. Sahoo and S. R. Samantaray, "An enhanced travelling wave-based fault detection and location estimation technique for series compensated transmission network," in *2017 7th International Conference on Power Systems (ICPS)*, 2017, pp. 61–68.

[13] B. Chaitanya and A. Yadav, "Decision tree aided travelling wave based fault section identification and location scheme for multi-terminal transmission lines," *Measurement*, vol. 135, pp. 312–322, 2019.

[14] M. Abedini, A. Hasani, A. H. Hajbabaie, and V. Khaligh, "A new traveling wave fault location algorithm in series compensated transmission line," in *2013 21st Iranian Conference on Electrical Engineering (ICEE)*, 2013, pp. 1–6.

[15] P. A. Crossley and P. G. McLaren, "Distance protection based on travelling waves," *IEEE Transactions on Power Apparatus and Systems*, vol. PAS-102, no. 9, pp. 2971–2983, Sep. 1983.

[16] E. H. Shehab-Eldin and P. G. McLaren, "Travelling wave distance protection-problem areas and solutions," *IEEE Transactions on Power Delivery*, vol. 3, no. 3, pp. 894–902, July 1988.

[17] V. Pathirana, P. G. McLaren, and E. Dirks, "Investigation of a hybrid travelling wave/impedance relay principle," in *IEEE CCECE2002. Canadian Conference on Electrical and Computer Engineering. Conference Proceedings (Cat. No.02CH37373)*, vol. 1, May 2002, pp. 48–53 vol.1.

[18] S. Marx, B. K. Johnson, A. Guzmán, V. Skendzic, and M. V. Mynam, "Traveling wave fault location in protective relays: Design, testing, and results," in *16th Annual Georgia Tech Fault and Disturbance Analysis Conference*, May 2013.

[19] S. Das, S. Santoso, A. Gaikwad, and M. Patel, "Impedance-based fault location in transmission networks: theory and application," *IEEE Access*, vol. 2, pp. 537–557, 2014.

[20] R. L. Reis and F. V. Lopes, "Correlation-based single-ended traveling wave fault location methods: A key settings parametric sensitivity analysis," *Electric Power Systems Research*, vol. 213, p. 108363, 2022.

[21] *Reason RPV311: Technical manual*, GE Grid Solutions, Norwalk, USA.

[22] E. O. Schweitzer III and V. Skendzic, "High-fidelity voltage measurement using resistive divider in a capacitance-coupled voltage transformer," Patent 20 190 094 287, March, 2019.